Determination of the $X(3872)$ Meson Quantum Numbers

R. Aaij *et al.**
(LHCb Collaboration)

(Received 25 February 2013; published 29 May 2013)

The quantum numbers of the $X(3872)$ meson are determined to be $J^{PC} = 1^{++}$ based on angular correlations in $B^+ \to X(3872)K^+$ decays, where $X(3872) \to \pi^+\pi^- J/\psi$ and $J/\psi \to \mu^+\mu^-$. The data correspond to 1.0 fb^{-1} of pp collisions collected by the LHCb detector. The only alternative assignment allowed by previous measurements $J^{PC} = 2^{-+}$ is rejected with a confidence level equivalent to more than 8 Gaussian standard deviations using a likelihood-ratio test in the full angular phase space. This result favors exotic explanations of the $X(3872)$ state.

DOI: 10.1103/PhysRevLett.110.222001 PACS numbers: 14.40.Rt, 13.25.Gv, 13.25.Hw, 14.40.Nd

It has been almost ten years since the narrow $X(3872)$ state was discovered in B^+ decays by the Belle experiment [1,2]. Subsequently, its existence has been confirmed by several other experiments [3–5]. Recently, its production has been studied at the LHC [6,7]. However, the nature of this state remains unclear. Among the open possibilities are conventional charmonium and exotic states such as $D^{*0}\bar{D}^0$ molecules [8], tetraquarks [9], or their mixtures [10]. Determination of the quantum numbers, total angular momentum J, parity P, and charge-conjugation C, is important to shed light on this ambiguity. The C parity of the state is positive since the $X(3872) \to \gamma J/\psi$ decay has been observed [11,12].

The CDF experiment analyzed three-dimensional (3D) angular correlations in a relatively high-background sample of 2292 ± 113 inclusively reconstructed $X(3872) \to \pi^+\pi^- J/\psi$, $J/\psi \to \mu^+\mu^-$ decays dominated by prompt production in $p\bar{p}$ collisions. The unknown polarization of the $X(3872)$ mesons limited the sensitivity of the measurement of J^{PC} [13]. A χ^2 fit of J^{PC} hypotheses to the binned 3D distribution of the J/ψ and $\pi\pi$ helicity angles ($\theta_{J/\psi}$, $\theta_{\pi\pi}$) [14–16] and the angle between their decay planes ($\Delta\phi_{J/\psi,\pi\pi} = \phi_{J/\psi} - \phi_{\pi\pi}$) excluded all spin-parity assignments except for 1^{++} or 2^{-+}. The Belle Collaboration observed 173 ± 16 $B \to X(3872)K$ ($K = K^\pm$ or K^0_S), $X(3872) \to \pi^+\pi^- J/\psi$, $J/\psi \to \ell^+\ell^-$ decays [17]. The reconstruction of the full decay chain resulted in a small background and polarized $X(3872)$ mesons, making their helicity angle (θ_X) and orientation of their decay plane (ϕ_X) sensitive to J^{PC} as well. By studying one-dimensional distributions in three different angles without exploiting correlations, they concluded that their data were equally well described by the 1^{++} and 2^{-+} hypotheses. The *BABAR* experiment observed 34 ± 7 $X(3872) \to \omega J/\psi$, $\omega \to \pi^+\pi^-\pi^0$ events [18]. The shape of observed $\pi^+\pi^-\pi^0$ mass distribution favored the 2^{-+} hypothesis, which had a confidence level (C.L.) of 62% over the 1^{++} hypothesis, but the latter was not ruled out (C.L. = 7%).

In this Letter, we report the first analysis of the complete five-dimensional angular correlations of the $B^+ \to X(3872)K^+$, $X(3872) \to \pi^+\pi^- J/\psi$, $J/\psi \to \mu^+\mu^-$ decay chain using $\sqrt{s} = 7$ TeV pp collision data corresponding to 1.0 fb^{-1} collected in 2011 by the LHCb experiment. The LHCb detector [19] is a single-arm forward spectrometer covering the pseudorapidity range $2 < \eta < 5$ designed for the study of particles containing b or c quarks. The detector includes a high precision tracking system consisting of a silicon-strip vertex detector surrounding the pp interaction region, a large-area silicon-strip detector located upstream of a dipole magnet with a bending power of about 4 Tm, and three stations of silicon-strip detectors and straw drift tubes placed downstream. The combined tracking system has momentum resolution $\Delta p/p$ that varies from 0.4% at 5 GeV to 0.6% at 100 GeV, and impact parameter resolution of 20 μm for tracks with high transverse momentum (p_T) [20]. Charged hadrons are identified using two ring-imaging Cherenkov detectors. Photon, electron, and hadron candidates are identified by a calorimeter system consisting of scintillating-pad and preshower detectors, an electromagnetic calorimeter, and a hadronic calorimeter. Muons are identified by a system composed of alternating layers of iron and multiwire proportional chambers. The trigger [21] consists of a hardware stage based on information from the calorimeter and muon systems followed by a software stage which applies a full event reconstruction.

In the off-line analysis, $J/\psi \to \mu^+\mu^-$ candidates are selected with the following criteria: $p_T(\mu) > 0.9$ GeV, $p_T(J/\psi) > 1.5$ GeV, χ^2 per degree of freedom for the two muons to form a common vertex, $\chi^2_{\rm vtx}(\mu^+\mu^-)/{\rm ndf} < 9$, and a mass consistent with the J/ψ meson. The separation of the J/ψ decay vertex from the nearest primary vertex (PV) must be at least 3 standard deviations.

*Full author list given at the end of the article.

Combinations of $K^+\pi^-\pi^+$ candidates that are consistent with originating from a common vertex with $\chi^2_{\rm vtx}(K^+\pi^-\pi^+)/{\rm ndf} < 9$, with each charged hadron (h) separated from all PVs [$\chi^2_{\rm IP}(h) > 9$] and having $p_{\rm T}(h) > 0.25$ GeV, are selected. The quantity $\chi^2_{\rm IP}(h)$ is defined as the difference between the χ^2 of the PV reconstructed with and without the considered particle. Kaon and pion candidates are required to satisfy $\ln[\mathcal{L}(K)/\mathcal{L}(\pi)] > 0$ and <5, respectively, where $\mathcal{L}$ is the particle identification likelihood [22]. If both same-sign hadrons in this combination meet the kaon requirement, only the particle with higher $p_{\rm T}$ is considered a kaon candidate. We combine J/ψ candidates with $K^+\pi^-\pi^+$ candidates to form B^+ candidates, which must satisfy $\chi^2_{\rm vtx}(J/\psi K^+\pi^-\pi^+)/{\rm ndf} < 9$, $p_{\rm T}(B^+) > 2$ GeV and have decay time greater than 0.25 ps. The $J/\psi K^+\pi^-\pi^+$ mass is calculated using the known J/ψ mass and the B vertex as constraints.

Four discriminating variables (x_i) are used in a likelihood ratio to improve the background suppression: the minimal $\chi^2_{\rm IP}(h)$, $\chi^2_{\rm vtx}(J/\psi K^+\pi^+\pi^-)/{\rm ndf}$, $\chi^2_{\rm IP}(B^+)$, and the cosine of the largest opening angle between the J/ψ and the charged-hadron transverse momenta. The latter peaks at positive values for the signal, as the B^+ meson has a high transverse momentum. Background events in which particles are combined from two different B decays peak at negative values, while those due to random combinations of particles are more uniformly distributed. The four 1D signal probability density functions (PDFs) $\mathcal{P}_{\rm sig}(x_i)$ are obtained from a simulated sample of $B^+ \to \psi(2S)K^+$, $\psi(2S) \to \pi^+\pi^- J/\psi$ decays, which are kinematically similar to the signal decays. The data sample of $B^+ \to \psi(2S)K^+$ events is used as a control sample for $\mathcal{P}_{\rm sig}(x_i)$ and for systematic studies in the angular analysis. The background PDFs $\mathcal{P}_{\rm bkg}(x_i)$ are obtained from the data in the B^+ mass sidebands (4.85–5.10 and 5.45–6.50 GeV). We require $-2\sum_{i=1}^{4} \ln[\mathcal{P}_{\rm sig}(x_i)/\mathcal{P}_{\rm bkg}(x_i)] < 1.0$, which preserves about 94% of the $X(3872)$ signal events.

About 38000 candidates are selected in a $\pm 2\sigma$ mass range around the B^+ peak in the $M(J/\psi\pi^+\pi^-K^+)$ distribution, with a signal purity of 89%. The $\Delta M = M(\pi^+\pi^- J/\psi) - M(J/\psi)$ distribution is shown in Fig. 1. Fits to the $\psi(2S)$ and $X(3872)$ signals are shown in the insets. A Crystal Ball function [23] with symmetric tails is used for the signal shapes. The background is assumed to be linear. The $\psi(2S)$ fit is performed in the 539.2–639.2 MeV range leaving all parameters free to vary. It yields 5642 ± 76 signal (230 ± 21 background) candidates with a ΔM resolution of $\sigma_{\Delta M} = 3.99 \pm 0.05$ MeV, corresponding to a signal purity of 99.2% within a $\pm 2.5\sigma_{\Delta M}$ region. When fitting in the 723–823 MeV range, the signal tail parameters are fixed to the values obtained in the $\psi(2S)$ fit, which also describe well the simulated $X(3872)$ signal distribution. The fit yields 313 ± 26 $B^+ \to X(3872)K^+$ candidates with a resolution of 5.5 ± 0.5 MeV. The number of background candidates

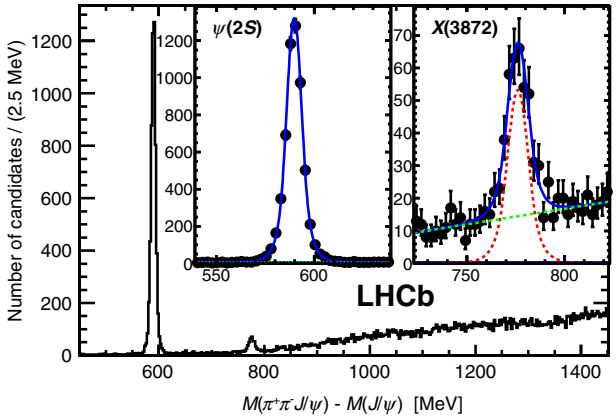

FIG. 1 (color online). Distribution of ΔM for $B^+ \to J/\psi K^+\pi^+\pi^-$ candidates. The fits of the $\psi(2S)$ and $X(3872)$ signals are displayed. The solid blue, dashed red, and dotted green lines represent the total fit, signal component, and background component, respectively.

is 568 ± 31 including the sideband regions. The signal purity is 68% within a $\pm 2.5\sigma_{\Delta M}$ signal region. The dominant source of background is from $B^+ \to J/\psi K_1(1270)^+$, $K_1(1270)^+ \to K^+\pi^+\pi^-$ decays, as found by studying the $K^+\pi^+\pi^-$ mass distribution.

The angular correlations in the B^+ decay carry information about the $X(3872)$ quantum numbers. To discriminate between the 1^{++} and 2^{-+} assignments, we use a likelihood-ratio test, which in general provides the most powerful discrimination between two hypotheses [24]. The PDF for each J^{PC} hypothesis J_X is defined in the 5D angular space $\Omega \equiv (\cos\theta_X, \cos\theta_{\pi\pi}, \Delta\phi_{X,\pi\pi}, \cos\theta_{J/\psi}, \Delta\phi_{X,J/\psi})$ by the normalized product of the expected decay matrix element ($\mathcal{M}$) squared and of the reconstruction efficiency (ϵ), $\mathcal{P}(\Omega|J_X) = |\mathcal{M}(\Omega|J_X)|^2\epsilon(\Omega)/I(J_X)$, where $I(J_X) = \int |\mathcal{M}(\Omega|J_X)|^2\epsilon(\Omega)d\Omega$. The efficiency is averaged over the $\pi^+\pi^-$ mass [$M(\pi\pi)$] using a simulation [25–29] that assumes the $X(3872) \to \rho(770)J/\psi$, $\rho(770) \to \pi^+\pi^-$ decay [7,17,30]. The observed $M(\pi\pi)$ distribution is in good agreement with this simulation. The line shape of the $\rho(770)$ resonance can change slightly depending on the spin hypothesis. The effect on $\epsilon(\Omega)$ is found to be very small and is neglected. We follow the approach adopted in Ref. [13] to predict the matrix elements. The angular correlations are obtained using the helicity formalism,

$$|\mathcal{M}(\Omega|J_X)|^2 = \sum_{\Delta\lambda_\mu=-1,+1} \Big| \sum_{\lambda_{J/\psi},\lambda_{\pi\pi}=-1,0,+1} A_{\lambda_{J/\psi},\lambda_{\pi\pi}} \times D^{J_X}_{0,\lambda_{J/\psi}-\lambda_{\pi\pi}}(\phi_X, \theta_X, -\phi_X) \times D^{1}_{\lambda_{\pi\pi},0}(\phi_{\pi\pi}, \theta_{\pi\pi}, -\phi_{\pi\pi}) \times D^{1}_{\lambda_{J/\psi},\Delta\lambda_\mu}(\phi_{J/\psi}, \theta_{J/\psi}, -\phi_{J/\psi}) \Big|^2,$$

where λ are particle helicities and $D^{J}_{\lambda_1,\lambda_2}$ are Wigner functions [14–16]. The helicity couplings $A_{\lambda_{J/\psi},\lambda_{\pi\pi}}$ are expressed in terms of the LS couplings [31,32], B_{LS}, where L is the orbital angular momentum between the $\pi\pi$ system and the J/ψ meson, and S is the sum of their spins. Since the energy release in the $X(3872) \to \rho(770)J/\psi$ decay is small, the lowest value of L is expected to dominate, especially because the next-to-minimal value is not allowed by parity conservation. The lowest value for the 1^{++} hypothesis is $L = 0$, which implies $S = 1$. With only one LS amplitude present, the angular distribution is completely determined without free parameters. For the 2^{-+} hypothesis, the lowest value is $L = 1$, which implies $S = 1$ or 2. As both LS combinations are possible, the 2^{-+} hypothesis implies two parameters, which are chosen to be the real and imaginary parts of $\alpha \equiv B_{11}/(B_{11} + B_{12})$. Since they are related to strong dynamics, they are difficult to predict theoretically and are treated as nuisance parameters.

We define a test statistic $t = -2\ln[\mathcal{L}(2^{-+})/\mathcal{L}(1^{++})]$, where the $\mathcal{L}(2^{-+})$ likelihood is maximized with respect to α. The efficiency $\epsilon(\Omega)$ is not determined on an event-by-event basis, since it cancels in the likelihood ratio except for the normalization integrals. A large sample of simulated events with uniform angular distributions passed through a full simulation of the detection and the data selection process is used to carry out the integration, $I(J_X) \propto \sum_{i=1}^{N_{\rm MC}} |\mathcal{M}(\Omega_i|J_X)|^2$, where $N_{\rm MC}$ is the number of reconstructed simulated events. The background in the data is subtracted in the log likelihoods using the sPlot technique [33] by assigning to each candidate in the fitted ΔM range an event weight (sWeight) w_i based on its ΔM value, $-2\ln\mathcal{L}(J_X) = -s_w 2\sum_{i=1}^{N_{\rm data}} w_i \ln\mathcal{P}(\Omega_i|J_X)$. Here, s_w is a constant scaling factor, $s_w = \sum_{i=1}^{N_{\rm data}} w_i / \sum_{i=1}^{N_{\rm data}} w_i^2$, which accounts for statistical fluctuations in the background subtraction. Positive (negative) values of the test statistic for the data $t_{\rm data}$ favor the 1^{++} (2^{-+}) hypothesis. The analysis procedure has been extensively tested on simulated samples for the 1^{++} and 2^{-+} hypotheses with different values of α generated using the EVTGEN package [27].

The value of α that minimizes $-2\ln\mathcal{L}(J_X = 2^{-+}, \alpha)$ in the data is $\hat{\alpha} = (0.671 \pm 0.046, 0.280 \pm 0.046)$. This is compatible with the value reported by Belle, (0.64,0.27) [17]. The value of the test statistic observed in the data is $t_{\rm data} = +99$, thus favoring the 1^{++} hypothesis. Furthermore, $\hat{\alpha}$ is consistent with the value of α obtained from fitting a large background-free sample of simulated 1^{++} events, $(0.650 \pm 0.011, 0.294 \pm 0.012)$. The value of $t_{\rm data}$ is compared with the distribution of t in the simulated experiments to determine a p value for the 2^{-+} hypothesis via the fraction of simulated experiments yielding a value of $t > t_{\rm data}$. We simulate 2 million experiments with the value of α, and the number of signal and background events, as observed in the data. The background is assumed to be saturated by the $B^+ \to J/\psi K_1(1270)^+$ decay, which provides a good description of its angular correlations. None of the values of t from the simulated experiments even approach $t_{\rm data}$, indicating a p value smaller than $1/(2 \times 10^6)$, which corresponds to a rejection of the 2^{-+} hypothesis with greater than 5σ significance. As shown in Fig. 2, the distribution of t is reasonably well approximated by a Gaussian function. Based on the mean and rms spread of the t distribution for the 2^{-+} experiments, this hypothesis is rejected with a significance of 8.4σ. The deviations of the t distribution from the Gaussian function suggest this is a plausible estimate. Using phase-space $B^+ \to J/\psi K^+\pi^+\pi^-$ decays as a model for the background events, we obtain a consistent result. The value of $t_{\rm data}$ falls into the region where the probability density for the 1^{++} simulated experiments is high. Integrating the 1^{++} distribution from $-\infty$ to $t_{\rm data}$ gives C.L.$(1^{++}) = 34\%$.

The value of t is the sum of the single-event likelihood ratios $\ln[\mathcal{P}(\Omega_i|2^{-+}, \hat{\alpha})/\mathcal{P}(\Omega_i|1^{++})]$ over the analyzed data sample and is therefore proportional to its average value. Even though this is the most effective way to discriminate between the two hypotheses, the agreement with the 1^{++} hypothesis might have been coincidental if the data were inconsistent with both tested hypotheses. However, the full shape of the single-event likelihood-ratio distribution also shows good consistency between the data and the distribution expected for the 1^{++} case, as illustrated in Fig. 3.

We vary the data selection criteria to probe for possible biases from the background subtraction and the efficiency corrections. The nominal selection does not bias the $M(\pi\pi)$ distribution. By requiring $Q = M(J/\psi\pi\pi) - M(J/\psi) - M(\pi\pi) < 0.1$ GeV, we reduce the background level by a factor of 4, while losing only 21% of the signal. The significance of the 2^{-+} rejection changes very little, in agreement with the simulations. By tightening the

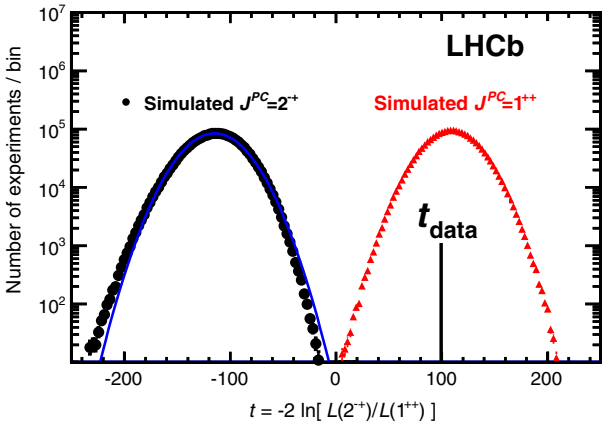

FIG. 2 (color online). Distribution of the test statistic t for the simulated experiments with $J^{PC} = 2^{-+}$ and $\alpha = \hat{\alpha}$ (black circles on the left) and with $J^{PC} = 1^{++}$ (red triangles on the right). A Gaussian fit to the 2^{-+} distribution is overlaid (blue solid line). The value of the test statistic for the data $t_{\rm data}$ is shown by the solid vertical line.

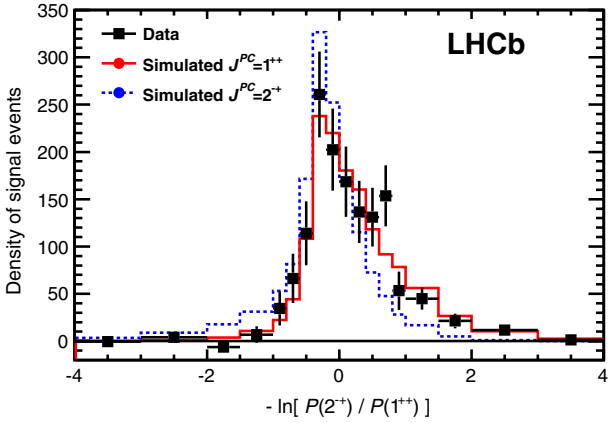

FIG. 3 (color online). Distribution of $-\ln[\mathcal{P}(\Omega_i|2^{-+},\hat{\alpha})/\mathcal{P}(\Omega_i|1^{++})]$ for the data (points with error bars) compared to the distributions for the simulated experiments with $J^{PC}=1^{++}$ (red solid histogram) and with $J^{PC}=2^{-+}$, $\alpha=\hat{\alpha}$ (blue dashed histogram) after the background subtraction using *sWeights*. The simulated distributions are normalized to the number of signal candidates observed in the data. Bin contents and uncertainties are divided by bin width because of unequal bin sizes.

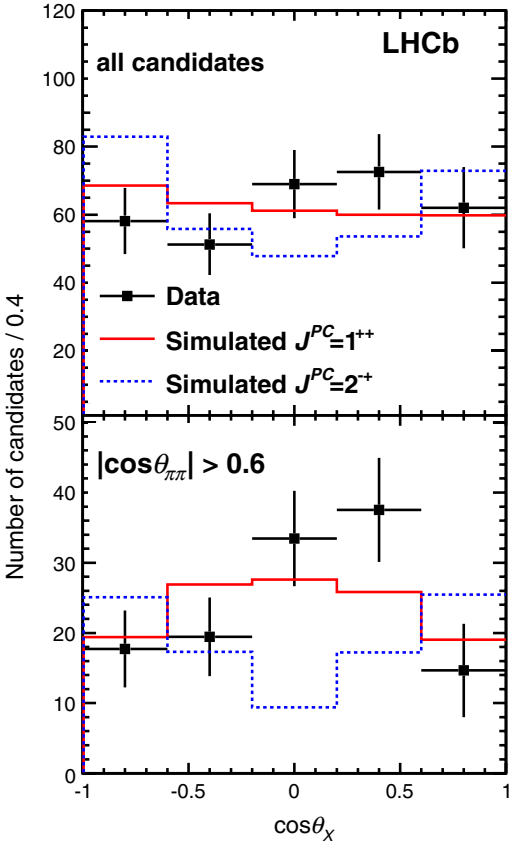

FIG. 4 (color online). Background-subtracted distribution of $\cos\theta_X$ for (top) all candidates and for (bottom) candidates with $|\cos\theta_{\pi\pi}|>0.6$ for the data (points with error bars) compared to the expected distributions for the $J^{PC}=1^{++}$ (red solid histogram) and $J^{PC}=2^{-+}$ and $\alpha=\hat{\alpha}$ hypotheses (blue dashed histogram). The simulated distributions are normalized to the number of signal candidates observed in the data across the full phase space.

requirements on the p_T of π, K, and μ candidates, we decrease the signal efficiency by about 50% with similar reduction in the background level. In all cases, the significance of the 2^{-+} rejection is reduced by a factor consistent with the simulations.

In the analysis we use simulations to calculate the $I(J_X)$ integrals. In an alternative approach to the efficiency estimates, we use the $B^+\to\psi(2S)K^+$ events observed in the data weighted by the inverse of 1^{--} matrix element squared. We obtain a value of $t_{\rm data}$ that corresponds to 8.2σ rejection of the 2^{-+} hypothesis.

As an additional goodness-of-fit test for the 1^{++} hypothesis, we project the data onto five 1D and ten 2D binned distributions in all five angles and their combinations. They are all consistent with the distributions expected for the 1^{++} hypothesis. Some of them are inconsistent with the distributions expected for the $(2^{-+},\hat{\alpha})$ hypothesis. The most significant inconsistency is observed for the 2D projections onto $\cos\theta_X$ vs $\cos\theta_{\pi\pi}$. The separation between the 1^{++} and 2^{-+} hypotheses increases when using correlations between these two angles, as illustrated in Fig. 4.

In summary, we unambiguously establish that the values of total angular momentum, parity, and charge-conjugation eigenvalues of the $X(3872)$ state are 1^{++}. This is achieved through the first analysis of the full five-dimensional angular correlations between final state particles in $B^+\to X(3872)K^+$, $X(3872)\to\pi^+\pi^- J/\psi$, $J/\psi\to\mu^+\mu^-$ decays using a likelihood-ratio test. The 2^{-+} hypothesis is excluded with a significance of more than 8 Gaussian standard deviations. This result rules out the explanation of the $X(3872)$ meson as a conventional $\eta_{c2}(1^1D_2)$ state. Among the remaining possibilities are the $\chi_{c1}(2^3P_1)$ charmonium disfavored by the value of the $X(3872)$ mass [34], and unconventional explanations such as a $D^{*0}\bar{D}^0$ molecule [8], tetraquark state [9], or charmonium-molecule mixture [10].

We express our gratitude to our colleagues in the CERN accelerator departments for the excellent performance of the LHC. We thank the technical and administrative staff at the LHCb institutes. We acknowledge support from CERN and from the following national agencies: CAPES, CNPq, FAPERJ, and FINEP (Brazil); NSFC (China); CNRS/IN2P3 and Region Auvergne (France); BMBF, DFG, HGF, and MPG (Germany); SFI (Ireland); INFN (Italy); FOM and NWO (Netherlands); SCSR (Poland); ANCS/IFA (Romania); MinES, Rosatom, RFBR, and NRC "Kurchatov Institute" (Russia); MinECo, XuntaGal, and GENCAT (Spain); SNSF and SER (Switzerland); NAS Ukraine (Ukraine); STFC (United Kingdom); NSF (USA). We also acknowledge the support received from the ERC under FP7. The Tier1 computing centers are

supported by IN2P3 (France), KIT and BMBF (Germany), INFN (Italy), NWO and SURF (Netherlands), PIC (Spain), and GridPP (United Kingdom). We are thankful for the computing resources put at our disposal by Yandex LLC (Russia), as well as to the communities behind the multiple open source software packages that we depend on.

[1] S.-K. Choi *et al.* (Belle Collaboration), Phys. Rev. Lett. **91**, 262001 (2003).
[2] The inclusion of charge-conjugate states is implied in this Letter.
[3] D. Acosta *et al.* (CDF Collaboration), Phys. Rev. Lett. **93**, 072001 (2004).
[4] V. M. Abazov *et al.* (D0 Collaboration), Phys. Rev. Lett. **93**, 162002 (2004).
[5] B. Aubert *et al.* (*BABAR* Collaboration), Phys. Rev. D **71**, 071103 (2005).
[6] R. Aaij *et al.* (LHCb Collaboration), Eur. Phys. J. C **72**, 1972 (2012).
[7] S. Chatrchyan *et al.* (CMS Collaboration), J. High Energy Phys. 04 (2013) 154.
[8] N. A. Tornqvist, Phys. Lett. B **590**, 209 (2004).
[9] L. Maiani, F. Piccinini, A. D. Polosa, and V. Riquer, Phys. Rev. D **71**, 014028 (2005).
[10] C. Hanhart, Y. Kalashnikova, and A. Nefediev, Eur. Phys. J. A **47**, 101 (2011).
[11] B. Aubert *et al.* (*BABAR* Collaboration), Phys. Rev. D **74**, 071101 (2006).
[12] V. Bhardwaj *et al.* (Belle Collaboration), Phys. Rev. Lett. **107**, 091803 (2011).
[13] A. Abulencia *et al.* (CDF Collaboration), Phys. Rev. Lett. **98**, 132002 (2007).
[14] M. Jacob and G. Wick, Ann. Phys. (Paris) **7**, 404 (1959).
[15] J. D. Richman, Report No. CALT-68-1148, 1984.
[16] S. U. Chung, Phys. Rev. D **57**, 431 (1998).
[17] S.-K. Choi *et al.* (Belle Collaboration), Phys. Rev. D **84**, 052004 (2011).
[18] P. del Amo Sanchez *et al.* (*BABAR* Collaboration), Phys. Rev. D **82**, 011101 (2010).
[19] A. A. Alves, Jr. *et al.* (LHCb Collaboration), JINST **3**, S08005 (2008).
[20] We use mass and momentum units in which $c = 1$.
[21] R. Aaij *et al.*, arXiv:1211.3055.
[22] M. Adinolfi *et al.*, arXiv:1211.6759.
[23] T. Skwarnicki, Ph.D. thesis, Institute of Nuclear Physics, Krakow, 1986 [DESY-F31-86-02].
[24] F. James, *Statistical Methods in Experimental Physics* (World Scientific Publishing, Singapore, 2006).
[25] T. Sjöstrand, S. Mrenna, and P. Skands, J. High Energy Phys. 05 (2006) 026.
[26] I. Belyaev *et al.* (LHCb Collaboration), J. Phys. Conf. Ser. **331**, 032047 (2011).
[27] D. J. Lange, Nucl. Instrum. Methods Phys. Res., Sect. A **462**, 52 (2001).
[28] J. Allison *et al.* (GEANT4 Collaboration), IEEE Trans. Nucl. Sci. **53**, 270 (2006); S. Agostinelli *et al.* (GEANT4 Collaboration), Nucl. Instrum. Methods Phys. Res., Sect. A **506**, 250 (2003).
[29] M. Clemencic, G. Corti, S. Easo, C. R. Jones, S. Miglioranzi, M. Pappagallo, and P. Robbe, J. Phys. Conf. Ser. **331**, 032023 (2011).
[30] A. Abulencia *et al.* (CDF Collaboration), Phys. Rev. Lett. **96**, 102002 (2006).
[31] J. Heuser, Ph.D. thesis, Universitat Karlsruhe, 2008 [IEKP-KA/2008-16].
[32] N. Mangiafave, Ph.D. thesis, University of Cambridge, 2012 [CERN-THESIS-2012-003].
[33] M. Pivk and F. R. Le Diberder, Nucl. Instrum. Methods Phys. Res., Sect. A **555**, 356 (2005).
[34] T. Skwarnicki, Int. J. Mod. Phys. A **19**, 1030 (2004).

R. Aaij,[40] C. Abellan Beteta,[35,n] B. Adeva,[36] M. Adinolfi,[45] C. Adrover,[6] A. Affolder,[51] Z. Ajaltouni,[5] J. Albrecht,[9] F. Alessio,[37] M. Alexander,[50] S. Ali,[40] G. Alkhazov,[29] P. Alvarez Cartelle,[36] A. A. Alves, Jr.,[24,37] S. Amato,[2] S. Amerio,[21] Y. Amhis,[7] L. Anderlini,[17,f] J. Anderson,[39] R. Andreassen,[59] R. B. Appleby,[53] O. Aquines Gutierrez,[10] F. Archilli,[18] A. Artamonov,[34] M. Artuso,[56] E. Aslanides,[6] G. Auriemma,[24,m] S. Bachmann,[11] J. J. Back,[47] C. Baesso,[57] V. Balagura,[30] W. Baldini,[16] R. J. Barlow,[53] C. Barschel,[37] S. Barsuk,[7] W. Barter,[46] Th. Bauer,[40] A. Bay,[38] J. Beddow,[50] F. Bedeschi,[22] I. Bediaga,[1] S. Belogurov,[30] K. Belous,[34] I. Belyaev,[30] E. Ben-Haim,[8] M. Benayoun,[8] G. Bencivenni,[18] S. Benson,[49] J. Benton,[45] A. Berezhnoy,[31] R. Bernet,[39] M. -O. Bettler,[46] M. van Beuzekom,[40] A. Bien,[11] S. Bifani,[12] T. Bird,[53] A. Bizzeti,[17,h] P. M. Bjørnstad,[53] T. Blake,[37] F. Blanc,[38] J. Blouw,[11] S. Blusk,[56] V. Bocci,[24] A. Bondar,[33] N. Bondar,[29] W. Bonivento,[15] S. Borghi,[53] A. Borgia,[56] T. J. V. Bowcock,[51] E. Bowen,[39] C. Bozzi,[16] T. Brambach,[9] J. van den Brand,[41] J. Bressieux,[38] D. Brett,[53] M. Britsch,[10] T. Britton,[56] N. H. Brook,[45] H. Brown,[51] I. Burducea,[28] A. Bursche,[39] G. Busetto,[21,q] J. Buytaert,[37] S. Cadeddu,[15] O. Callot,[7] M. Calvi,[20,j] M. Calvo Gomez,[35,n] A. Camboni,[35] P. Campana,[18,37] A. Carbone,[14,c] G. Carboni,[23,k] R. Cardinale,[19,i] A. Cardini,[15] H. Carranza-Mejia,[49] L. Carson,[52] K. Carvalho Akiba,[2] G. Casse,[51] M. Cattaneo,[37] Ch. Cauet,[9] M. Charles,[54] Ph. Charpentier,[37] P. Chen,[30,3] N. Chiapolini,[39] M. Chrzaszcz,[25] K. Ciba,[37] X. Cid Vidal,[36] G. Ciezarek,[52] P. E. L. Clarke,[49] M. Clemencic,[37] H. V. Cliff,[46] J. Closier,[37] C. Coca,[28] V. Coco,[40] J. Cogan,[6] E. Cogneras,[5] P. Collins,[37] A. Comerma-Montells,[35] A. Contu,[15] A. Cook,[45] M. Coombes,[45] S. Coquereau,[8] G. Corti,[37] B. Couturier,[37] G. A. Cowan,[38] D. Craik,[47] S. Cunliffe,[52] R. Currie,[49] C. D'Ambrosio,[37] P. David,[8] P. N. Y. David,[40] I. De Bonis,[4] K. De Bruyn,[40] S. De Capua,[53] M. De Cian,[39] J. M. De Miranda,[1]

M. De Oyanguren Campos,[35,o] L. De Paula,[2] W. De Silva,[59] P. De Simone,[18] D. Decamp,[4] M. Deckenhoff,[9] L. Del Buono,[8] D. Derkach,[14] O. Deschamps,[5] F. Dettori,[41] A. Di Canto,[11] H. Dijkstra,[37] M. Dogaru,[28] S. Donleavy,[51] F. Dordei,[11] A. Dosil Suárez,[36] D. Dossett,[47] A. Dovbnya,[42] F. Dupertuis,[38] R. Dzhelyadin,[34] A. Dziurda,[25] A. Dzyuba,[29] S. Easo,[48,37] U. Egede,[52] V. Egorychev,[30] S. Eidelman,[33] D. van Eijk,[40] S. Eisenhardt,[49] U. Eitschberger,[9] R. Ekelhof,[9] L. Eklund,[50] I. El Rifai,[5] Ch. Elsasser,[39] D. Elsby,[44] A. Falabella,[14,e] C. Färber,[11] G. Fardell,[49] C. Farinelli,[40] S. Farry,[12] V. Fave,[38] D. Ferguson,[49] V. Fernandez Albor,[36] F. Ferreira Rodrigues,[1] M. Ferro-Luzzi,[37] S. Filippov,[32] C. Fitzpatrick,[37] M. Fontana,[10] F. Fontanelli,[19,i] R. Forty,[37] O. Francisco,[2] M. Frank,[37] C. Frei,[37] M. Frosini,[17,f] S. Furcas,[20] E. Furfaro,[23] A. Gallas Torreira,[36] D. Galli,[14,c] M. Gandelman,[2] P. Gandini,[54] Y. Gao,[3] J. Garofoli,[56] P. Garosi,[53] J. Garra Tico,[46] L. Garrido,[35] C. Gaspar,[37] R. Gauld,[54] E. Gersabeck,[11] M. Gersabeck,[53] T. Gershon,[47,37] Ph. Ghez,[4] V. Gibson,[46] V. V. Gligorov,[37] C. Göbel,[57] D. Golubkov,[30] A. Golutvin,[52,30,37] A. Gomes,[2] H. Gordon,[54] M. Grabalosa Gándara,[5] R. Graciani Diaz,[35] L. A. Granado Cardoso,[37] E. Graugés,[35] G. Graziani,[17] A. Grecu,[28] E. Greening,[54] S. Gregson,[46] O. Grünberg,[58] B. Gui,[56] E. Gushchin,[32] Yu. Guz,[34] T. Gys,[37] C. Hadjivasiliou,[56] G. Haefeli,[38] C. Haen,[37] S. C. Haines,[46] S. Hall,[52] T. Hampson,[45] S. Hansmann-Menzemer,[11] N. Harnew,[54] S. T. Harnew,[45] J. Harrison,[53] T. Hartmann,[58] J. He,[7] V. Heijne,[40] K. Hennessy,[51] P. Henrard,[5] J. A. Hernando Morata,[36] E. van Herwijnen,[37] E. Hicks,[51] D. Hill,[54] M. Hoballah,[5] C. Hombach,[53] P. Hopchev,[4] W. Hulsbergen,[40] P. Hunt,[54] T. Huse,[51] N. Hussain,[54] D. Hutchcroft,[51] D. Hynds,[50] V. Iakovenko,[43] M. Idzik,[26] P. Ilten,[12] R. Jacobsson,[37] A. Jaeger,[11] E. Jans,[40] P. Jaton,[38] F. Jing,[3] M. John,[54] D. Johnson,[54] C. R. Jones,[46] B. Jost,[37] M. Kaballo,[9] S. Kandybei,[42] M. Karacson,[37] T. M. Karbach,[37] I. R. Kenyon,[44] U. Kerzel,[37] T. Ketel,[41] A. Keune,[38] B. Khanji,[20] O. Kochebina,[7] I. Komarov,[38,31] R. F. Koopman,[41] P. Koppenburg,[40] M. Korolev,[31] A. Kozlinskiy,[40] L. Kravchuk,[32] K. Kreplin,[11] M. Kreps,[47] G. Krocker,[11] P. Krokovny,[33] F. Kruse,[9] M. Kucharczyk,[20,25,j] V. Kudryavtsev,[33] T. Kvaratskheliya,[30,37] V. N. La Thi,[38] D. Lacarrere,[37] G. Lafferty,[53] A. Lai,[15] D. Lambert,[49] R. W. Lambert,[41] E. Lanciotti,[37] G. Lanfranchi,[18,37] C. Langenbruch,[37] T. Latham,[47] C. Lazzeroni,[44] R. Le Gac,[6] J. van Leerdam,[40] J. -P. Lees,[4] R. Lefèvre,[5] A. Leflat,[31,37] J. Lefrançois,[7] S. Leo,[22] O. Leroy,[6] B. Leverington,[11] Y. Li,[3] L. Li Gioi,[5] M. Liles,[51] R. Lindner,[37] C. Linn,[11] B. Liu,[3] G. Liu,[37] J. von Loeben,[20] S. Lohn,[37] J. H. Lopes,[2] E. Lopez Asamar,[35] N. Lopez-March,[38] H. Lu,[3] D. Lucchesi,[21,q] J. Luisier,[38] H. Luo,[49] F. Machefert,[7] I. V. Machikhiliyan,[4,30] F. Maciuc,[28] O. Maev,[29,37] S. Malde,[54] G. Manca,[15,d] G. Mancinelli,[6] U. Marconi,[14] R. Märki,[38] J. Marks,[11] G. Martellotti,[24] A. Martens,[8] L. Martin,[54] A. Martín Sánchez,[7] M. Martinelli,[40] D. Martinez Santos,[41] D. Martins Tostes,[2] A. Massafferri,[1] R. Matev,[37] Z. Mathe,[37] C. Matteuzzi,[20] E. Maurice,[6] A. Mazurov,[16,32,37,e] J. McCarthy,[44] R. McNulty,[12] A. Mcnab,[53] B. Meadows,[59,54] F. Meier,[9] M. Meissner,[11] M. Merk,[40] D. A. Milanes,[8] M. -N. Minard,[4] J. Molina Rodriguez,[57] S. Monteil,[5] D. Moran,[53] P. Morawski,[25] M. J. Morello,[22,s] R. Mountain,[56] I. Mous,[40] F. Muheim,[49] K. Müller,[39] R. Muresan,[28] B. Muryn,[26] B. Muster,[38] P. Naik,[45] T. Nakada,[38] R. Nandakumar,[48] I. Nasteva,[1] M. Needham,[49] N. Neufeld,[37] A. D. Nguyen,[38] T. D. Nguyen,[38] C. Nguyen-Mau,[38,p] M. Nicol,[7] V. Niess,[5] R. Niet,[9] N. Nikitin,[31] T. Nikodem,[11] A. Nomerotski,[54] A. Novoselov,[34] A. Oblakowska-Mucha,[26] V. Obraztsov,[34] S. Oggero,[40] S. Ogilvy,[50] O. Okhrimenko,[43] R. Oldeman,[15,37,d] M. Orlandea,[28] J. M. Otalora Goicochea,[2] P. Owen,[52] B. K. Pal,[56] A. Palano,[13,b] M. Palutan,[18] J. Panman,[37] A. Papanestis,[48] M. Pappagallo,[50] C. Parkes,[53] C. J. Parkinson,[52] G. Passaleva,[17] G. D. Patel,[51] M. Patel,[52] G. N. Patrick,[48] C. Patrignani,[19,i] C. Pavel-Nicorescu,[28] A. Pazos Alvarez,[36] A. Pellegrino,[40] G. Penso,[24,l] M. Pepe Altarelli,[37] S. Perazzini,[14,c] D. L. Perego,[20,j] E. Perez Trigo,[36] A. Pérez-Calero Yzquierdo,[35] P. Perret,[5] M. Perrin-Terrin,[6] G. Pessina,[20] K. Petridis,[52] A. Petrolini,[19,i] A. Phan,[56] E. Picatoste Olloqui,[35] B. Pietrzyk,[4] T. Pilař,[47] D. Pinci,[24] S. Playfer,[49] M. Plo Casasus,[36] F. Polci,[8] G. Polok,[25] A. Poluektov,[47,33] E. Polycarpo,[2] D. Popov,[10] B. Popovici,[28] C. Potterat,[35] A. Powell,[54] J. Prisciandaro,[38] V. Pugatch,[43] A. Puig Navarro,[38] G. Punzi,[22,r] W. Qian,[4] J. H. Rademacker,[45] B. Rakotomiaramanana,[38] M. S. Rangel,[2] I. Raniuk,[42] N. Rauschmayr,[37] G. Raven,[41] S. Redford,[54] M. M. Reid,[47] A. C. dos Reis,[1] S. Ricciardi,[48] A. Richards,[52] K. Rinnert,[51] V. Rives Molina,[35] D. A. Roa Romero,[5] P. Robbe,[7] E. Rodrigues,[53] P. Rodriguez Perez,[36] S. Roiser,[37] V. Romanovsky,[34] A. Romero Vidal,[36] J. Rouvinet,[38] T. Ruf,[37] F. Ruffini,[22] H. Ruiz,[35] P. Ruiz Valls,[35,o] G. Sabatino,[24,k] J. J. Saborido Silva,[36] N. Sagidova,[29] P. Sail,[50] B. Saitta,[15,d] C. Salzmann,[39] B. Sanmartin Sedes,[36] M. Sannino,[19,i] R. Santacesaria,[24] C. Santamarina Rios,[36] E. Santovetti,[23,k] M. Sapunov,[6] A. Sarti,[18,l] C. Satriano,[24,m] A. Satta,[23] M. Savrie,[16,e] D. Savrina,[30,31] P. Schaack,[52] M. Schiller,[41] H. Schindler,[37] M. Schlupp,[9] M. Schmelling,[10] B. Schmidt,[37] O. Schneider,[38] A. Schopper,[37] M. -H. Schune,[7] R. Schwemmer,[37] B. Sciascia,[18] A. Sciubba,[24] M. Seco,[36] A. Semennikov,[30] K. Senderowska,[26] I. Sepp,[52] N. Serra,[39] J. Serrano,[6] P. Seyfert,[11] M. Shapkin,[34] I. Shapoval,[42,37] P. Shatalov,[30] Y. Shcheglov,[29] T. Shears,[51,37]

L. Shekhtman,[33] O. Shevchenko,[42] V. Shevchenko,[30] A. Shires,[52] R. Silva Coutinho,[47] T. Skwarnicki,[56] N. A. Smith,[51] E. Smith,[54,48] M. Smith,[53] M. D. Sokoloff,[59] F. J. P. Soler,[50] F. Soomro,[18,37] D. Souza,[45] B. Souza De Paula,[2] B. Spaan,[9] A. Sparkes,[49] P. Spradlin,[50] F. Stagni,[37] S. Stahl,[11] O. Steinkamp,[39] S. Stoica,[28] S. Stone,[56] B. Storaci,[39] M. Straticiuc,[28] U. Straumann,[39] V. K. Subbiah,[37] S. Swientek,[9] V. Syropoulos,[41] M. Szczekowski,[27] P. Szczypka,[38,37] T. Szumlak,[26] S. T'Jampens,[4] M. Teklishyn,[7] E. Teodorescu,[28] F. Teubert,[37] C. Thomas,[54] E. Thomas,[37] J. van Tilburg,[11] V. Tisserand,[4] M. Tobin,[39] S. Tolk,[41] D. Tonelli,[37] S. Topp-Joergensen,[54] N. Torr,[54] E. Tournefier,[4,52] S. Tourneur,[38] M. T. Tran,[38] M. Tresch,[39] A. Tsaregorodtsev,[6] P. Tsopelas,[40] N. Tuning,[40] M. Ubeda Garcia,[37] A. Ukleja,[27] D. Urner,[53] U. Uwer,[11] V. Vagnoni,[14] G. Valenti,[14] R. Vazquez Gomez,[35] P. Vazquez Regueiro,[36] S. Vecchi,[16] J. J. Velthuis,[45] M. Veltri,[17,g] G. Veneziano,[38] M. Vesterinen,[37] B. Viaud,[7] D. Vieira,[2] X. Vilasis-Cardona,[35,n] A. Vollhardt,[39] D. Volyanskyy,[10] D. Voong,[45] A. Vorobyev,[29] V. Vorobyev,[33] C. Voß,[58] H. Voss,[10] R. Waldi,[58] R. Wallace,[12] S. Wandernoth,[11] J. Wang,[56] D. R. Ward,[46] N. K. Watson,[44] A. D. Webber,[53] D. Websdale,[52] M. Whitehead,[47] J. Wicht,[37] J. Wiechczynski,[25] D. Wiedner,[11] L. Wiggers,[40] G. Wilkinson,[54] M. P. Williams,[47,48] M. Williams,[55] F. F. Wilson,[48] J. Wishahi,[9] M. Witek,[25] S. A. Wotton,[46] S. Wright,[46] S. Wu,[3] K. Wyllie,[37] Y. Xie,[49,37] F. Xing,[54] Z. Xing,[56] Z. Yang,[3] R. Young,[49] X. Yuan,[3] O. Yushchenko,[34] M. Zangoli,[14] M. Zavertyaev,[10,a] F. Zhang,[3] L. Zhang,[56] W. C. Zhang,[12] Y. Zhang,[3] A. Zhelezov,[11] A. Zhokhov,[30] L. Zhong,[3] and A. Zvyagin[37]

(LHCb Collaboration)

[1]*Centro Brasileiro de Pesquisas Físicas (CBPF), Rio de Janeiro, Brazil*
[2]*Universidade Federal do Rio de Janeiro (UFRJ), Rio de Janeiro, Brazil*
[3]*Center for High Energy Physics, Tsinghua University, Beijing, People's Republic of China*
[4]*LAPP, Université de Savoie, CNRS/IN2P3, Annecy-Le-Vieux, France*
[5]*Clermont Université, Université Blaise Pascal, CNRS/IN2P3, LPC, Clermont-Ferrand, France*
[6]*CPPM, Aix-Marseille Université, CNRS/IN2P3, Marseille, France*
[7]*LAL, Université Paris-Sud, CNRS/IN2P3, Orsay, France*
[8]*LPNHE, Université Pierre et Marie Curie, Université Paris Diderot, CNRS/IN2P3, Paris, France*
[9]*Fakultät Physik, Technische Universität Dortmund, Dortmund, Germany*
[10]*Max-Planck-Institut für Kernphysik (MPIK), Heidelberg, Germany*
[11]*Physikalisches Institut, Ruprecht-Karls-Universität Heidelberg, Heidelberg, Germany*
[12]*School of Physics, University College Dublin, Dublin, Ireland*
[13]*Sezione INFN di Bari, Bari, Italy*
[14]*Sezione INFN di Bologna, Bologna, Italy*
[15]*Sezione INFN di Cagliari, Cagliari, Italy*
[16]*Sezione INFN di Ferrara, Ferrara, Italy*
[17]*Sezione INFN di Firenze, Firenze, Italy*
[18]*Laboratori Nazionali dell'INFN di Frascati, Frascati, Italy*
[19]*Sezione INFN di Genova, Genova, Italy*
[20]*Sezione INFN di Milano Bicocca, Milano, Italy*
[21]*Sezione INFN di Padova, Padova, Italy*
[22]*Sezione INFN di Pisa, Pisa, Italy*
[23]*Sezione INFN di Roma Tor Vergata, Roma, Italy*
[24]*Sezione INFN di Roma La Sapienza, Roma, Italy*
[25]*Henryk Niewodniczanski Institute of Nuclear Physics Polish Academy of Sciences, Kraków, Poland*
[26]*AGH University of Science and Technology, Kraków, Poland*
[27]*National Center for Nuclear Research (NCBJ), Warsaw, Poland*
[28]*Horia Hulubei National Institute of Physics and Nuclear Engineering, Bucharest-Magurele, Romania*
[29]*Petersburg Nuclear Physics Institute (PNPI), Gatchina, Russia*
[30]*Institute of Theoretical and Experimental Physics (ITEP), Moscow, Russia*
[31]*Institute of Nuclear Physics, Moscow State University (SINP MSU), Moscow, Russia*
[32]*Institute for Nuclear Research of the Russian Academy of Sciences (INR RAN), Moscow, Russia*
[33]*Budker Institute of Nuclear Physics (SB RAS) and Novosibirsk State University, Novosibirsk, Russia*
[34]*Institute for High Energy Physics (IHEP), Protvino, Russia*
[35]*Universitat de Barcelona, Barcelona, Spain*
[36]*Universidad de Santiago de Compostela, Santiago de Compostela, Spain*
[37]*European Organization for Nuclear Research (CERN), Geneva, Switzerland*
[38]*Ecole Polytechnique Fédérale de Lausanne (EPFL), Lausanne, Switzerland*

[39]*Physik-Institut, Universität Zürich, Zürich, Switzerland*
[40]*Nikhef National Institute for Subatomic Physics, Amsterdam, Netherlands*
[41]*Nikhef National Institute for Subatomic Physics and VU University Amsterdam, Amsterdam, Netherlands*
[42]*NSC Kharkiv Institute of Physics and Technology (NSC KIPT), Kharkiv, Ukraine*
[43]*Institute for Nuclear Research of the National Academy of Sciences (KINR), Kyiv, Ukraine*
[44]*University of Birmingham, Birmingham, United Kingdom*
[45]*H.H. Wills Physics Laboratory, University of Bristol, Bristol, United Kingdom*
[46]*Cavendish Laboratory, University of Cambridge, Cambridge, United Kingdom*
[47]*Department of Physics, University of Warwick, Coventry, United Kingdom*
[48]*STFC Rutherford Appleton Laboratory, Didcot, United Kingdom*
[49]*School of Physics and Astronomy, University of Edinburgh, Edinburgh, United Kingdom*
[50]*School of Physics and Astronomy, University of Glasgow, Glasgow, United Kingdom*
[51]*Oliver Lodge Laboratory, University of Liverpool, Liverpool, United Kingdom*
[52]*Imperial College London, London, United Kingdom*
[53]*School of Physics and Astronomy, University of Manchester, Manchester, United Kingdom*
[54]*Department of Physics, University of Oxford, Oxford, United Kingdom*
[55]*Massachusetts Institute of Technology, Cambridge, Massachusetts, USA*
[56]*Syracuse University, Syracuse, New York, USA*
[57]*Pontifícia Universidade Católica do Rio de Janeiro (PUC-Rio), Rio de Janeiro, Brazil [associated with Universidade Federal do Rio de Janeiro (UFRJ), Rio de Janeiro, Brazil]*
[58]*Institut für Physik, Universität Rostock, Rostock, Germany (associated with Physikalisches Institut, Ruprecht-Karls-Universität Heidelberg, Heidelberg, Germany)*
[59]*University of Cincinnati, Cincinnati, Ohio, USA (associated with Syracuse University, Syracuse, New York, USA)*

[a]P.N. Lebedev Physical Institute, Russian Academy of Science (LPI RAS), Moscow, Russia.
[b]Università di Bari, Bari, Italy.
[c]Università di Bologna, Bologna, Italy.
[d]Università di Cagliari, Cagliari, Italy.
[e]Università di Ferrara, Ferrara, Italy.
[f]Università di Firenze, Firenze, Italy.
[g]Università di Urbino, Urbino, Italy.
[h]Università di Modena e Reggio Emilia, Modena, Italy.
[i]Università di Genova, Genova, Italy.
[j]Università di Milano Bicocca, Milano, Italy.
[k]Università di Roma Tor Vergata, Roma, Italy.
[l]Università di Roma La Sapienza, Roma, Italy.
[m]Università della Basilicata, Potenza, Italy.
[n]LIFAELS, La Salle, Universitat Ramon Llull, Barcelona, Spain.
[o]IFIC, Universitat de Valencia-CSIC, Valencia, Spain.
[p]Hanoi University of Science, Hanoi, Vietnam.
[q]Università di Padova, Padova, Italy.
[r]Università di Pisa, Pisa, Italy.
[s]Scuola Normale Superiore, Pisa, Italy.